Fresnel Zone to Far Field Algorithm for Rapid Array Antenna Measurements

M. Sierra-Castañer , S. Burgos

Abstract— **This paper presents the implementation of a Fresnel zone to far field transformation algorithm [1-2] for the measurements of the main patterns (E and H plane) of separable array antennas, from the acquired field values in those main patterns. The method is based on the Fourier Series decomposition of the $1/R^2$ term of the field propagation in spherical coordinates. This method is valid for Fresnel Zone Measurements, where the $1/R^3$ term can be neglected. The Antenna Test Facility of the Technical University of Madrid (LEHA-UPM) is using this method for characterizing the BTS antennas for GSM and UMTS cellular systems. These antennas have dual linear polarization (±45º), several antenna ports (depending on the antenna design) and a controlled electrical downtilt, typically from 0º to 14º. Antenna manufacturers and cellular companies are normally interested in the radiation pattern for the main planes, so this method is applied to reduce drastically the acquisition time with accurate results.**

I. Introduction

The acquisition time is becoming more and more important in the characterization of the commercial antennas. In particular, one of the challenges of the Antenna Test Facility of the Technical University of Madrid ("Laboratorio de Ensayos y Homologación de Antenas LEHA-UPM") is the measurement in a very reduced time of the base station antennas (Fig. 1) for GSM, UMTS or other cellular systems. These antennas are larger and larger and include several ports for dual polarization and different frequency bands. Also, they have to be measured for different electrical tilt configurations. Of course, the antennas have to be measured at a large number of frequencies to assure a good performance in the whole frequency band. The positive aspect is that the users are mainly interested in the main patterns and in the most important antenna parameters (peak gain, losses, horizontal and vertical beamwidth, tilt in the vertical plane and squint in the horizontal planes). The measurements in far field require large chambers for these antennas and frequencies ($r>2D^2/\lambda$) while the measurements in traditional spherical near field systems require a complete acquisition, that means unaffordable times. This paper presents the application of an algorithm based on the Fourier Series decomposition of the $1/R^2$ term of the field propagation in spherical coordinates, introduced in [1-4], and called discrete beam sampling method (DBSM) for Wu. This method is valid for Fresnel Zone Measurements (1), where the $1/R^3$ term can be neglected.

$$r > 0.62\sqrt{\frac{D^3}{\lambda}} \tag{1}$$

This algorithm was first used for the characterization of ASAR panels of ENVISAT satellite in 1995, and then it has been updated for the measurement of this kind of antennas.

The paper presents the algorithm, the first application for the ASAR panels and the results for the SATIMO BTS1940 antenna, a reference antenna for the measurements of BTS antennas. These results are compared, in gain and pattern with the standard spherical near to far field transformation using the TICRA software SNIFTD. The conclusion will be summarized the validity of this method.

Fig. 1 Example of BTS Antenna for GSM and UMTS.

II. SPHERICAL FRESNEL ZONE TO FAR FIELD ALGORITHM (SFIFT)

The algorithm is based on the assumption than the $1/R^3$ term can be neglected in Fresnel zone and far field distances (1). This technique is applicable to linear antennas or apertures and arrays with separable distribution. The measurement time can be drastically reduced with respect to near field techniques since just the measurement of the main patterns is required. However, only the far field radiation pattern in the principal planes can be calculated, from the Fresnel zone acquisition in the principal patterns.

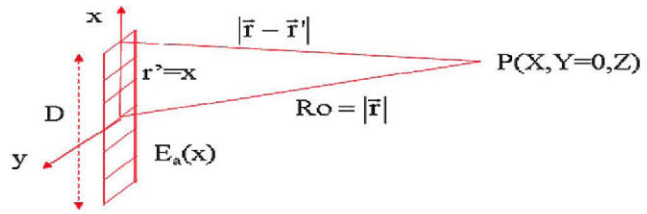

Fig. 2 Radiating linear strip.

The radiated field generated by a linear strip (Fig. 2) in the point P can be written as (2):

$$E = C\int E_a(x)\frac{e^{-jk_o|\vec{r}-\vec{r}'|}}{|\vec{r}-\vec{r}'|}dx \qquad (2)$$

where C is a constant value. In (2), the distance between the radiating element and the observation point, if the y coordinates of the observation and source point are 0 (same plane), is:

$$|\vec{r}-\vec{r}'| \approx R_o - x\cdot sen\theta + \frac{1}{2R_o}x^2\cos^2\theta - \frac{1}{2R_o^{\,2}}x^3 sen\theta\cdot\cos^2\theta \qquad (3)$$

Far field condition approximates the expression (3) by the linear term, neglecting the quadratic and cubic term (4) and (5).

$$E_{ff} = C\int_{-D/2}^{D/2} E_a(x)e^{jk_o x\sin\theta}dx = C\int_{-1}^{1} E_a\left(\frac{x}{D/2}\right)e^{jk_o\frac{x\cdot D/2}{D/2}\sin\theta}d\left(\frac{x}{D/2}\right)$$

$$= C\int_{-1}^{1} E_a(x_n)e^{j\frac{\pi}{\lambda}x_n\cdot D\sin\theta}dx_n = \int_{-1}^{1} E_a(x_n)e^{jux_n}dx_n \qquad (4)$$

where λ represents the wavelength, D stands for the length of the antenna in x direction, x_n is equal to $x/(D/2)$ and u is equal to $\pi D sin\theta/\lambda$.

However, in Fresnel Zone condition (1), with a smaller measurement distance R_o, the quadratic term must be considered while the cubic term can be suppressed. In this case, the acquired field can be approximated as:

$$E_{R_o}(u) = C\int_{-1}^{1} E_a(x_n)e^{jux_n}e^{-j\alpha_{Ro}x_n^{\,2}}dx_n \qquad (5)$$

where $\alpha_{Ro} = \frac{\pi\cos^2\theta}{8\beta_{Ro}}$ and $\beta_{Ro} = \frac{R_o}{2D^2/\lambda}$ is the ratio between the measurement distance (R_o) and the far field distance ($2D^2/\lambda$).

The far field (4) can be expressed as:

$$E_{ff} = C\int_{-1}^{1} E_a(x_n)e^{jux_n}\cdot e^{-j\alpha_{Ro}x_n^{\,2}}\cdot e^{j\alpha_{Ro}x_n^{\,2}}dx_n \qquad (6)$$

If the exponential term is replaced by its Fourier series decomposition:

$$e^{j\alpha_{Ro}x_n^{\,2}} = \sum_{n=-N}^{N} A_n e^{jn\pi x_n} \qquad (7)$$

then, the far field can be expressed as a summitry of integral terms (8)

$$E_{ff} = C\sum_{n=-N}^{N} A_n\int_{-1}^{1} E_a(x_n)e^{j(u+n\pi)x_n}e^{-j\alpha_{Ro}x_n^{\,2}}dx_n \qquad (8)$$

The coefficients A_n are calculated inverting (7),

$$A_n = \frac{1}{2}\int_{-1}^{1} e^{j\alpha_{Ro}x_n^{\,2}}\cdot e^{-jn\pi x_n}dx_n \qquad (9)$$

Therefore, the far field can be expressed in terms of the measured field in Fresnel Zone (10):

$$E_{ff} = \sum_{n=-N}^{N} A_n E_{Ro}(u+n\pi) \qquad (10)$$

The results depend on a right selection of the parameter N. The algorithm was validated through simulations for a rectangular antenna of Dx = 1 m, Dy = 0.5 m, at a frequency of 6 GHz with cosine illumination. In this case the far field distance ($2D^2/\lambda$) is 40 meters and the simulated measurement distance is 5.5 meters. The compared results are shown in Fig. 3. In this case, Fresnel Zone is 2.77 meters, so the AUT is clearly inside this area.

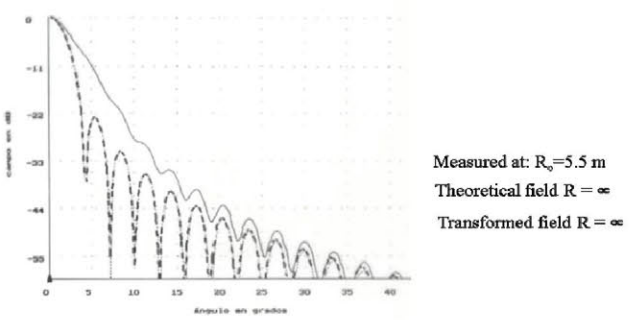

Fig. 3 Simulations for a rectangular aperture: theoretical and transformed far field and acquired field at 5.5 meters.

The second simulated case was for a linear strip of D = 1 m at 6 GHz with uniform illumination In this case the far field distance ($2D^2/\lambda$) is 40 meters and the simulated measurement

distance is 5.5 meters. The compared results are shown in Fig. 4. In this case, the simulated measured is a 2.7 meters, just in the limit of the Fresnel Zone (2.77 meters)

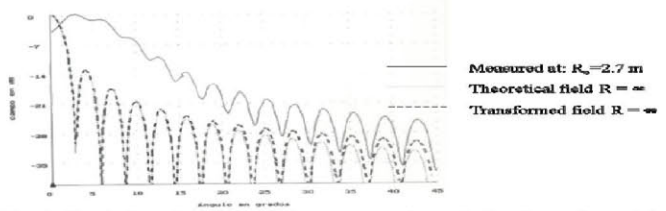

Fig. 4 Simulations for a rectangular aperture: theoretical and transformed far field and acquired field at 2.7 meters.

The software used in the LEHA-UPM facilities was first applied for the measurement of the array panels of the ASAR (Fig. 6) antenna (ENVISAT satellite – Fig. 5).

Fig. 5 ENVISAT satellite.

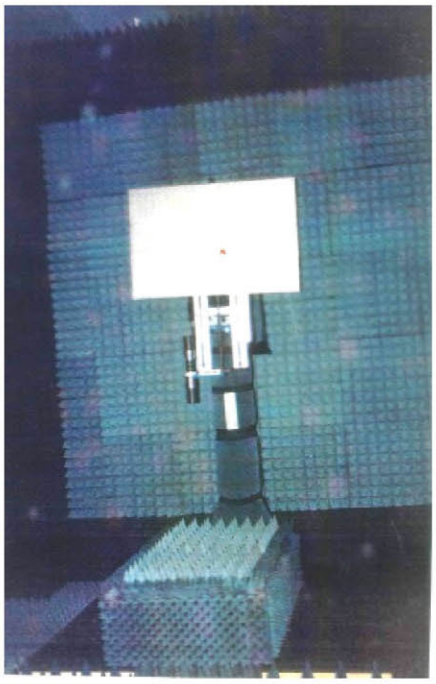

Fig. 6 ASAR panel of the ENVISAT satellite in LEHA-UPM facility.

A panel was measured using the previous transformation algorithm (SFIFT) and the SNIFTD (spherical to far field transformation software by TICRA [5]) in order to validate the algorithm through measurements. The results at 5.5 meters (1/8 of the far field distance) are shown in Fig. 7 and Fig. 8 for the main patterns.

As it can be observed, the agreements are very good. Finally, these panels were measured using the proposed algorithm.

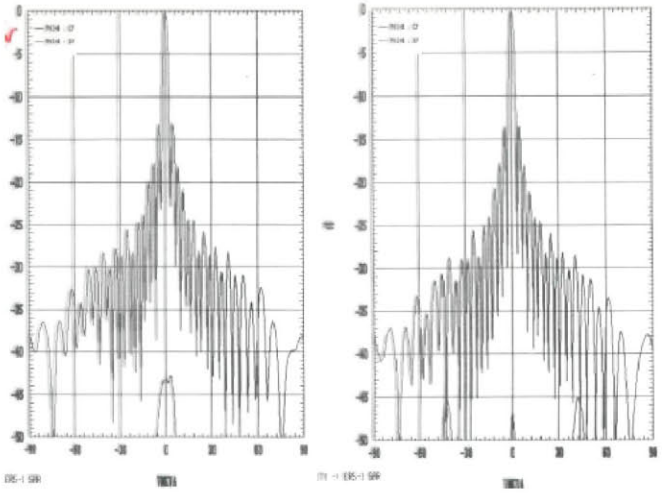

Fig. 7 Horizontal plane of the ASAR panel of the ENVISAT satellite in LEHA-UPM facility: SFIFT (left) and SNIFTD (right)

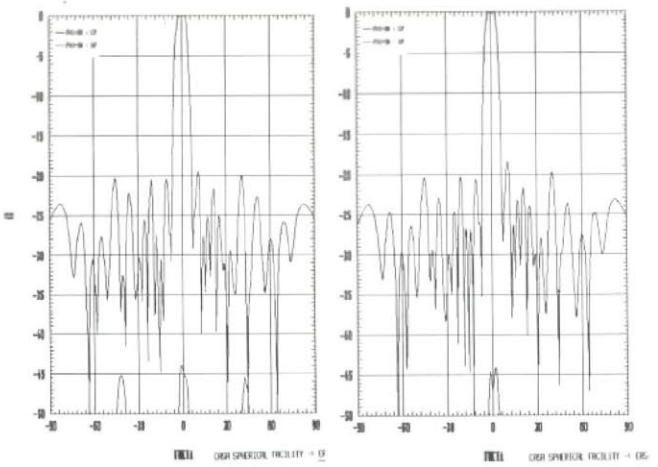

Fig. 8 Vertical plane of the ASAR panel of the ENVISAT satellite in LEHA-UPM facility: SFIFT (left) and SNIFTD (right)

III. Application to BTS Antennas

The BTS antennas are each time more and more complex. Nowadays the BTS antennas work in very wide frequency bands (790–960 and 1710–2690 MHz) to cover all the bands assigned to cellular systems and with high gains. Also, there are several antennas included in the same radome, all of them

with dual polarization (typically linear slant ±45º). Finally, the antenna patterns can be electronically tilted within a very wide angular range (up to 0º to 14º). Also, the radiation patterns have to follow strict specifications, as it is shown with an example in Fig. 9.

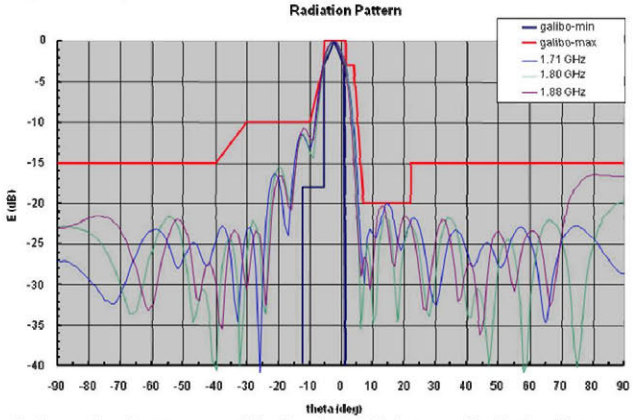

Fig. 9 Example of pattern specification for BTS Antenna Radiation Pattern.

All this makes the measurement time a very important factor. Table I shows the measurement distance and the number of patterns (directly related with the measurement time) for the three cases: measurement in far field ($2D^2/\lambda$), in Fresnel region $0.62(D^3/\lambda)^{1/2}$ and in near field (6λ). This is done for different BTS antenna cases. The number of patterns is 2 for far field and Fresnel zone and $N=k_oD/2+10$ for the case of spherical near field. It is observed that Fresnel Zone is much better in distance with respect to the far field case and in measurement time with respect to the spherical near field case.

TABLE I
MEASUREMENT DISTANCE AND NUMBERS OF PATTERNS FOR FAR FIELD MEASUREMENT, FRESNEL ZONE AND SPHERICAL NEAR FIELD

Antenna		Far Field		Fresnel Zone		Sph Near Field	
		Dist (m)	*Cuts*	*Dist (m)*	*Cuts*	*Dist (m)*	*Cuts*
GSM900	**L=1.5 m**	14,4	2	1,9	2	2,0	25
GSM900	**L=2.2 m**	31,0	2	1,9	2	3,6	32
UMTS	**L=1.5 m**	32,6	2	0,8	2	3,1	44
UMTS	**L=2.2 m**	70,0	2	0,8	2	5,4	60

However, for this application a variation in the algorithm was developed. This was due to the fact that the previous algorithm just calculates the far field in half ring (-90º to 90º). For this application, the process is repeated for the back and front half circumference and both patterns are combined using an interpolation in the border zone. Also, a good selection of the number of periods (N in eq. 10) is required. In this case, a low value of N is better for the crosspolar and for the back radiation. For the horizontal plane, since the beamwidth is high, also a low value of N can be selected for the copolar pattern. The main drawback of the method is that the AUT has to be aligned with the centre of rotation of the azimuth positioner, so for wider antennas (more than one antenna in the radome), a special set-up for moving the AUT is required.

This method is being used by LEHA-UPM for measuring BTS antennas for Telefonica and Vodafone.

IV. VALIDATION OF THE ALGORITHM WITH THE SATIMO BTS1940 REFERENCE ANTENNA.

In 2009, UPM participated in a new intercomparison campaign supported by SATIMO. In this case, the AUT is a BTS array working in GSM1800 and UMTS frequency bands (1710 to 2170 MHz). The BTS1940 is a linear array reference antenna with dual slant +45°/-45° or H/V polarized. This antenna is ideal as reference for calibration of antenna measurement systems. The array is specifically designed to achieve excellent cross-polar discrimination and to maintain a well-defined radiation pattern in the direction of the boresight axis throughout the operational bandwidth. The BTS1940 antennas are equipped with high precision female N type connectors for superior repeatability and durability. The nominal impedance is 50 Ohm with return loss values better than -15 dB (VSWR < 1.5). UPM measured this antenna in the spherical near field system using a full sphere acquisition and transforming to far field with the SNIFTD software and this algorithm (SFIFT).

Fig. 10: SATIMO linear array antenna 1710-2170MHz (BTS1940) in test configuration.

In order to compare both transformation processes, some values are extracted. The calculated values are:

- For the gain: the difference in the IEEE peak gain for both procedures. The important results are the mean (indicator of the systematic error) and the standard deviation (indicator of the uncertainty).
- For the on-axis directivity: the same results.
- For the radiation pattern: the weighted average logarithmic difference of both patterns, using the procedure shown in Pivnenko et al [6]. In this comparison the noise level is -60dB and the parameter β=0.25. The mean of this value is an indicator of the uncertainty.

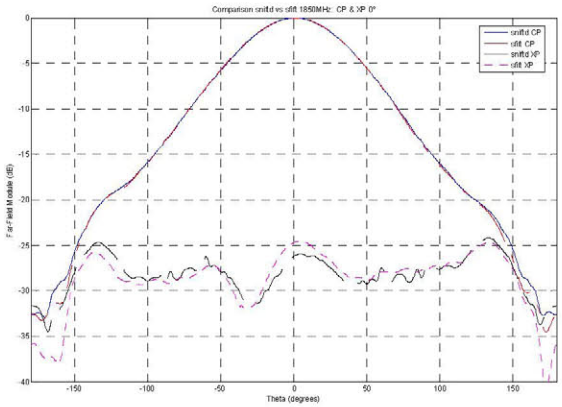

Fig. 11: Horizontal plane antenna pattern comparison at 1850 MHz

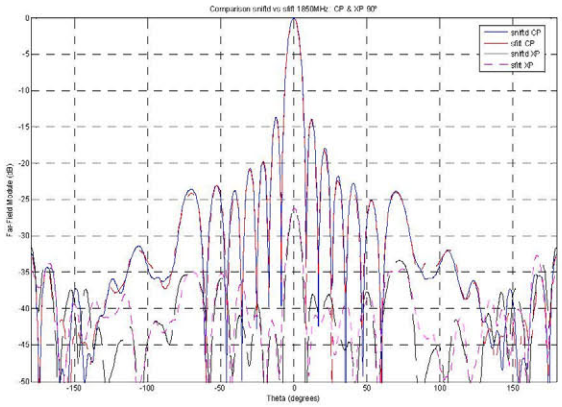

Fig. 12: Vertical plane antenna pattern comparison at 1850 MHz

TABLE II
DIFFERENCES IN PEAK GAIN, PEAK DIRECTIVIY AND WEIGHTED PATTERN BETWEEN SNIFTD AND PROPOSED ALGORTIHM (SFIFT)

FREQ (MHz)	Gain errors (dB)	Dir Errors (dB)	Pattern uncertainty (dB)
1500	0,15	0,25	0,08
1600	-0,02	0,18	0,11
1710	-0,08	0,17	0,09
1795	0,25	0,12	0,10
1850	0,10	0,16	0,09
1880	0,15	0,15	0,10
1920	0,14	0,12	0,09
2045	0,30	0,04	0,11
2170	0,29	-0,14	0,10
2200	0,24	-0,14	0,11
2300	0,25	-0,09	0,12
Mean	0,16	0,07	0,10
Std. Deviation	0,12	0,14	

These results show that SFIFT slightly overestimates the on-axis gain and directivity. Since the SGH gain, the reflection coefficient and the acquired on-axis field of BTS and SGH have been achieved just once, these results are representative of the transformation errors of SFIFT (assuming that the transformation error of SNIFTD is negligible). It is remarkable than the peak directivity, in the case of SFIFT, is just an approximate value obtained from the two principal planes.

Fig. 11 and Fig. 12 show the comparisons between the complete acquisition and the SFIFT software for the principal planes. The measurement distance is always 5.5 meters (in Fresnel Zone). The results are very good both in copolar and in crosspolar components.

V. CONCLUSIONS

This paper has presented the application of a method developed some years ago (called discrete beam sampling method DBSM) for array antennas. The method was first checked with simulations and used for the measurements of the ASAR antennas of the ENVISAT satellite.

Nowadays, this method has been completed to be able to measure the pattern in the complete ring. This allows us to measure the BTS antennas for GSM or UMTS networks, and in fact, it is being used for Telefonica or Vodafone.

The validation process, with comparison with a near field acquisition and a transformation to far field using SNIFTD has been presented, showing a very good agreement.

ACKNOWLEDGMENT

The authors want to thank the Spanish Government for the support of this work under the projects SEMSYT (TSI-020100-2010-194) of AVANZA2 program and the project PTQ-10-03307 of Torres Quevedo program.

REFERENCES

[1] Marlborg, L. Hansson. "Quasi far-field to far field transformation". Proc. 11th ESTEC Workshop on Antenna Measurements, June 1988.

[2] K. Wu and S. Parekh. "Methods of transforming antenna Fresnel region fields to far region fields". Proc. AMTA Monterrey, CA. October 1989. Pp. 11.9 to 11.14

[3] Evans, Gary E. "Antenna Measurement Techniques". Artech House, 1990.

[4] C. Rivas, J.L. Besada, J. Rodrigo. "Simulación de medidas de antenas en zona de Fresnel y transformación a campo lejano". Proc. VIII Symposium Nacional URSI. Valencia. Sept. 1993.

[5] SNIFTD Software by TICRA. www.ticra.com

[6] S. Pivnenko, J.E. Pallesen, O. Breinbjerg, M. Sierra-Castañer, P. Caballero, C. Martínez, J.L. Besada, J. Romeu, S. Blanch, J.M. González-Arbesu, C. Sabatier, A. Calderone, G. Portier, H. Eriksson, J. Zackrisson. "Comparison of Antenna Measurement Facilities With the DTU-ESA 12 GHz Validation Standard Antenna Within the EU Antenna Centre of Excellence". IEEE TAP. July 2009. Vol. 57. N. 7. Pp. 1863- 1878.